Acta Crystallographica Section F
Structural Biology and Crystallization Communications
ISSN 1744-3091

Structure of the wild-type human BCL6 POZ domain

Mark A. Stead,[a]‡ Gareth O. Rosbrook,[a]‡ Jonathan M. Hadden,[b] Chi H. Trinh,[b] Stephen B. Carr[b]§ and Stephanie C. Wright[a]*

[a]Molecular Cell Biology Research Group, Garstang/Astbury Buildings, Institute of Molecular and Cellular Biology, Faculty of Biological Sciences, University of Leeds, Leeds LS2 9JT, England, and [b]Astbury Centre for Structural Molecular Biology, Garstang/Astbury Buildings, Institute of Molecular and Cellular Biology, Faculty of Biological Sciences, University of Leeds, Leeds LS2 9JT, England

‡ These authors contributed equally to this work.
§ Present address: Membrane Protein Laboratory, Diamond Light Source, Harwell Science and Innovation Campus, Chilton, Didcot OX11 0DE, England.

Correspondence e-mail: s.c.wright@leeds.ac.uk

Received 17 October 2008
Accepted 3 November 2008

PDB Reference: BCL6 POZ domain, 3e4u, r3e4usf.

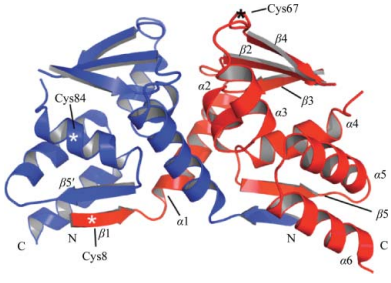

BCL6 is a transcriptional repressor that is overexpressed in diffuse large B-cell lymphoma and follicular lymphoma. The N-terminal POZ domain of BCL6 interacts with transcriptional corepressors and targeting these associations is a promising therapeutic strategy. Previous structural studies of the BCL6 POZ domain have used a mutant form because of the low solubility of the wild-type recombinant protein. A method for the purification and crystallization of the wild-type BCL6 POZ domain is described and the crystal structure to 2.1 Å resolution is reported. This will be relevant for the design of therapeutics that target BCL6 POZ-domain interaction interfaces.

1. Introduction

BCL6 (B-cell lymphoma 6) is a zinc-finger transcription factor that regulates B-cell development (Chang *et al.*, 1996). It is expressed at high levels in germinal centre B cells (Cattoretti *et al.*, 1995), where somatic hypermutation and class-switch recombination of the immunoglobulin genes lead to the production of high-affinity antibodies. In this setting, BCL6 represses the transcription of genes that control cell-cycle arrest, apoptosis, differentiation and the DNA-damage response, thereby enabling the rapid proliferation of germinal centre B cells that are undergoing DNA deletions and mutations (Baron *et al.*, 1997; Phan & Dalla-Favera, 2004; Parekh *et al.*, 2007; Ranuncolo *et al.*, 2007). The expression of BCL6 is crucially downregulated at the end of the germinal centre (GC) reaction, thus allowing the differentiation of B cells into plasma cells and memory B cells. Chromosome translocations and mutations affecting the promoter of the BCL6 gene are observed in diffuse large B-cell lymphoma (DLBCL) and follicular lymphoma (FL) (Baron *et al.*, 1993; Kerckaert *et al.*, 1993; Ye *et al.*, 1993, 1995); the resulting overexpression of BCL6 blocks the differentiation and apoptosis of B cells, leading to their retention at the proliferative GC stage. Targeting BCL6 function is a promising therapeutic strategy for some DLBCL patients (Chattopadhyay *et al.*, 2006; Parekh *et al.*, 2008; Polo *et al.*, 2004).

The N-terminal POZ/BTB (poxvirus and zinc finger/bric-à-brac, tramtrack and broad complex) domain of BCL6 mediates many of its transcriptional properties. The POZ domain is a conserved protein–protein interaction motif that is found in approximately 40 zinc-finger transcription factors (POZ-ZF factors; reviewed in Stogios *et al.*, 2005). Most POZ-ZF factors have roles in development and many are implicated as oncogenes or tumour suppressors in human cancer (reviewed in Kelly & Daniel, 2006); for example, PLZF (promyelocytic leukaemia zinc finger; Chen *et al.*, 1993), BCL6 and LRF (leukaemia/lymphoma-related factor; Maeda *et al.*, 2005) are involved in specific types of leukaemia and lymphoma. POZ domains direct the oligomerization of POZ-ZF factors and also mediate the recruitment of transcriptional coregulators and other non-POZ partners (Huynh & Bardwell, 1998). POZ-ZF factors are thought to function as biological dimers and crystal structures of the PLZF (Ahmad *et al.*, 1998; Li *et al.*, 1999), BCL6 (Ahmad *et al.*, 2003; Ghetu *et al.*, 2008) and LRF (Schubot *et al.*, 2006; Stogios *et al.*, 2007) POZ domains revealed domain-swapped homodimers with a conserved

BTB fold. Higher order oligomers and heteromeric interactions of POZ-ZF factors are also biologically important and some of the activities of BCL6 are mediated by a POZ–POZ interaction between BCL6 and the POZ-ZF factor Miz-1 (Phan *et al.*, 2005). The stoichiometries of heteromeric POZ-domain complexes are unknown. The recent crystal structure of the Miz-1 POZ domain (Stead *et al.*, 2007) revealed a tetrameric organization in which two POZ dimers interact *via* the solvent-exposed β-sheets located along one surface. This β-sheet interface mediates the tetramerization of the Miz-1 POZ domain in solution and may be a candidate for mediating the higher order association and hetero-oligomerization of other POZ-ZF factors.

The BCL6 POZ domain recruits the transcriptional corepressors BCoR (BCL6-interacting corepressor), SMRT (silencing mediator for retinoid and thyroid hormone receptors) and NCoR (nuclear receptor corepressor) in a mutually exclusive manner by recognition of the 17-residue BBD (BTB-binding domain) region of the corepressors. No BBD motif exists at the sequence level; although the SMRT and NCoR BBD sequences are highly conserved, the BCoR BBD shares no similarity with either. Crystal structures of the BCL6 POZ domain in complex with SMRT or BCoR BBD peptides showed that these corepressors use very different determinants for recognition of the same binding surface of the BTB dimer (Ahmad *et al.*, 2003; Ghetu *et al.*, 2008). Peptides that mimic either the SMRT or BCoR BBDs led to the killing of BCL6-positive DLBCL tumour cells, indicating potential therapeutic applications.

All reported crystal structures of the BCL6 POZ domain represent a mutant protein in which three surface cysteine residues were altered in order to enhance solubility and to aid the purification of recombinant protein. Since these mutations are located in regions that may be involved in either POZ-domain oligomerization or the recruitment of other factors, it is advantageous to additionally determine the structure of the wild-type protein. We present a method for the purification and crystallization of the wild-type BCL6 POZ domain and report the crystal structure to 2.1 Å resolution.

2. Materials and methods

2.1. Cloning

A DNA fragment encoding the BCL6 POZ domain (BCL6 residues 5–129) was amplified from a human placental cDNA library and inserted into pGEX-6P-1 (GE Healthcare). The resulting plasmid encoded a fusion protein containing an N-terminal glutathione *S*-transferase (GST) tag and a PreScission protease cleavage site.

2.2. Protein expression and purification

Protocols for expression of the recombinant wild-type BCL6 POZ domain were optimized to specifically increase the proportion of protein obtained in the soluble fraction. GST-fusion proteins were expressed in *Escherichia coli* Rosetta (DE3) pLysS (Novagen). Bacteria were cultured at 310 K to an $OD_{600\,nm}$ of 0.6 in 2TY broth supplemented with 0.3% ethanol (Steczko *et al.*, 1991). Cells were cooled rapidly on ice and recombinant protein expression was induced with 0.1 m*M* IPTG at 289 K for 16 h. Bacterial pellets were resuspended in PBS, 0.1% Triton X-100, 5 m*M* DTT pH 7.5; inclusion of 5 m*M* DTT in all buffers was essential for recombinant protein stability and subsequent purification. Cells were lysed by sonication and fusion proteins were bound to glutathione-Sepharose 4B (GE Healthcare). The GST tag was subsequently removed by cleavage with PreScission protease in 20 m*M* Tris–HCl, 75 m*M* NaCl, 5 m*M* DTT pH 7.5. The BCL6 POZ domain was further purified by anion-exchange chromatography on Resource Q in 10 m*M* Tris–HCl, 50 m*M* NaCl, 5 m*M* DTT pH 8.5 and eluted with a 50–300 m*M* NaCl gradient. This was followed by size-exclusion chromatography on a Superdex 75 HiLoad 26/60 column (GE Healthcare). The protein was eluted in 20 m*M* Tris–HCl, 250 m*M* NaCl, 5 m*M* DTT, 5% glycerol pH 8.5 and concentrated to 4.5 mg ml^{-1} using Amicon centrifugal concentrators (Millipore).

Table 1
Data-collection and processing statistics.

Values in parentheses are for the highest resolution shell.

Crystal parameters	
Space group	$P3_2$
Unit-cell parameters (Å, °)	a = 59.21, b = 59.21, c = 158.97, α = 90, β = 90, γ = 120
Data collection	
Resolution (Å)	36.86–2.10 (2.21–2.10)
Wavelength (Å)	0.972
R_{merge}† (%)	6.8 (15.7)
$R_{p.i.m.}$‡ (%)	4.0 (9.2)
$\langle I/\sigma(I)\rangle$	16.3 (4.6)
No. of unique reflections	36195
Multiplicity	3.8 (3.9)
Completeness (%)	99.4 (100)
Twinning	
Twin fraction	
Twin operator h, k, l	0.539
Twin operator $-h$, $h + k$, $-l$	0.461
Refinement	
Resolution (Å)	2.1
R§ (%)	21.9
R_{free}¶ (%)	25.9
R.m.s.d. stereochemistry††	
Bond lengths (Å)	0.011
Bond angles (°)	1.294
No. of protein atoms	5827
No. of water molecules	256
Average B factor (Å^2)	33.169
Ramachandran analysis‡‡ (%)	
Favoured	97.3
Allowed	100.0
Disallowed	0

† $R_{merge} = \sum_{hkl}\sum_i |I_i(hkl) - \langle I(hkl)\rangle|/\sum_{hkl}\sum_i I_i(hkl)$, where $I_i(hkl)$ is the integrated intensity of a given reflection and $\langle I(hkl)\rangle$ is the mean intensity of multiple corresponding symmetry-related reflections. ‡ $R_{pim} = \sum_{hkl}[1/(N-1)]^{1/2}\sum_i |I_i(hkl) - \langle I(hkl)\rangle|/\sum_{hkl}\sum_i I_i(hkl)$, where $I_i(hkl)$ is the integrated intensity of a given reflection, $\langle I(hkl)\rangle$ is the mean intensity of multiple corresponding symmetry-related reflections and N is the multiplicity of a given reflection. § $R = \sum_{hkl}||F_o|_{hkl} - |F_c|_{hkl}|/\sum_{hkl}|F_o|_{hkl}$, where F_o and F_c are the observed and calculated structure factors, respectively. ¶ R_{free} is R calculated using 5% random data excluded from the refinement. †† R.m.s.d. stereochemistry is the deviation from ideal values. ‡‡ Ramachandran analysis was carried out using *MolProbity* (Davis *et al.*, 2007).

2.3. Crystallization

Crystals of the BCL6 POZ domain were grown at 291 K using sitting-drop vapour diffusion by mixing 2 µl protein solution (4.5 mg ml^{-1}) with 3 µl reservoir solution (2.5 *M* $NaNO_3$, 100 m*M* sodium acetate pH 4.5, 40 m*M* spermidine). Large hexagonal crystals were typically obtained after 48 h. Crystals were mounted in a nylon CryoLoop (Hampton Research) and transferred into mother liquor supplemented with 17.5% glycerol for 30 s before being flash-frozen in liquid nitrogen.

2.4. Data collection, structure determination and refinement

X-ray diffraction data were collected under a nitrogen-gas stream at 100 K at the Diamond Synchrotron Light Source (Didcot, UK), beamline I04. Data reduction was performed using *iMOSFLM* and *SCALA* (Collaborative Computational Project, Number 4, 1994; Leslie, 1992). The cumulative intensity distribution calculated within *TRUNCATE* (French & Wilson, 1978) suggested the data were

twinned. This was confirmed by the generation of Britton plots (Britton, 1972) within the program *DETWIN* (Rees, 1980), which revealed a twin fraction of 46%. Matthews analysis (Kantardjieff & Rupp, 2003) suggested the presence of three BCL6 dimers within the asymmetric unit and native Patterson maps calculated using detwinned data displayed peaks that suggested that the three dimers were related by translational NCS. Initial phase estimates were generated using the molecular-replacement program *AMoRe* (Navaza, 2001), using a mutant BCL6 POZ domain (Ahmad *et al.*, 2003; PDB code 1r28) as the search model. The asymmetric unit contained three POZ-domain dimers related by purely translational NCS that were positioned sequentially. The final model was built by iterative model building in *Coot* (Emsley & Cowtan, 2004) and twinned refinement using *REFMAC* v.5.5 (Murshudov *et al.*, 1997). Stereochemistry was analysed with the *PROCHECK* (Laskowski *et al.*, 1993) and *MolProbity* (Davis *et al.*, 2007) programs. Structure superpositions were calculated using the *SUPERPOSE* server (Maiti *et al.*, 2004) and images of protein structures were prepared using *PyMOL* (DeLano, 2002).

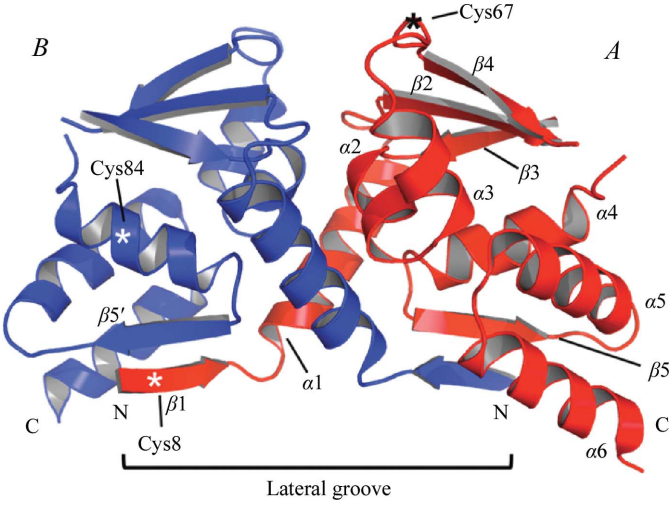

Figure 1
Ribbon representation of the wild-type BCL6 POZ-domain dimer. Subunits *A* and *B* are shown in red and blue, respectively, and the secondary-structure elements of the *A* chain and of the $\beta1$–$\beta5'$ interface are labelled (positions of the *B* chain are indicated by primes). Residues Cys8, Cys67 and Cys84 were mutated in previously reported BCL6 POZ-domain structures and are indicated by asterisks. The lateral groove has been shown to mediate the recruitment of corepressors SMRT and BCoR (Ahmad *et al.*, 2003; Ghetu *et al.*, 2008).

3. Results and discussion

The wild-type human BCL6 POZ domain (BCL6 residues 5–129) was expressed in *E. coli*, purified and crystallized. The crystals were merohedrally twinned and the asymmetric unit contained three POZ-domain dimers that were related by translational NCS. The structure was solved by molecular replacement and refined to R = 21.9%, $R_{\rm free}$ = 25.9% at 2.1 Å resolution (Table 1, Fig. 1).

The organization of the wild-type BCL6 POZ domain is the same as previously reported POZ-domain dimers, with each subunit containing a core of α-helices that is flanked at the top and bottom by β-sheets (described according to the orientation depicted in Fig. 1). The dimerization interface comprises a central region consisting of α-helices, together with two two-stranded β-sheets ($\beta1$–$\beta5'$) that lie at the bottom of the molecule. The N-termini of the subunits are exchanged to yield a domain-swapped dimer in which each β-sheet of the dimerization interface contains a strand derived from each subunit. Compared with the wild-type BCL6 POZ domain, the r.m.s.d. values of C^{α}-atom positions for the reported mutant BCL6 POZ domains are 1.5 Å (PDB code 1r2b), 0.97 Å (1r28), 1.10 Å (1r29) (Ahmad *et al.*, 2003) and 1.12 Å (3bim; Ghetu *et al.*, 2008); in comparison, similar superposition of 1r29 with other BCL6 POZ-domain structures yields r.m.s.d. values of 1.08 Å (1r2b), 0.92 Å (1r28) and 1.13 Å (3bim).

Previously reported BCL6 POZ-domain structures represent proteins that contain mutations of three cysteine residues (C8Q, C67R and C84N) to enhance the solubility and the purification of the recombinant protein. These cysteine residues are not conserved between POZ domains of different POZ-ZF factors. Cys8 is located in the N-terminal $\beta1$ strand that forms part of the POZ-domain dimerization interface, Cys67 is in the unstructured loop between $\alpha3$ and $\beta4$ and Cys84 is in $\alpha4$ on the outside of the dimer.

The side chains of Cys8, Cys67 and Cys84 in the wild-type BCL6 POZ domain are solvent-exposed (Figs. 1 and 2); the $\beta1$ Cys8 and $\alpha4$ Cys84 side chains of opposite subunits of the domain-swapped dimer point outwards from the same face of the molecule. The $\beta1$–$\beta5'$ sheets of the reported mutant (C8Q,C67R,C84N) BCL6 POZ domains form approximately 35% of the dimerization interface; there is no substantial main-chain deviation between the wild-type and mutant structures in this region (Fig. 2). The $\beta1$–$\beta5'$ sheet also plays a crucial role in the recruitment of the corepressors SMRT and BCoR, which interact with the lateral groove that runs along the bottom of the dimer and extends into the dimerization interface (Ahmad *et al.*, 2003; Ghetu *et al.*, 2008). Two molecules of corepressor interact with the POZ-domain dimer and each contributes a lower third strand to

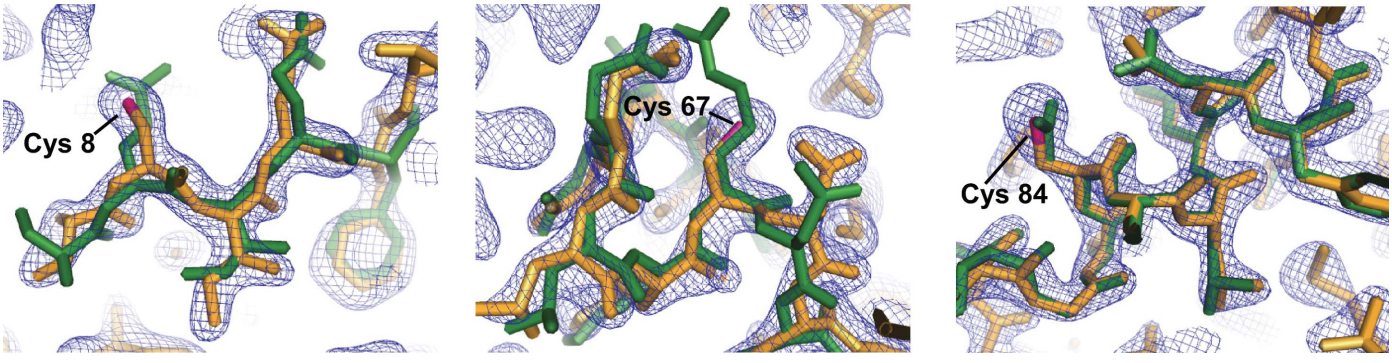

Figure 2
Comparison of wild-type and mutant BCL6 POZ-domain structures. The residues surrounding Cys8, Cys67 and Cys84 are shown in a stick representation. The wild-type BCL6 POZ domain (ochre) is superposed with the corresponding region from the reported mutant (green; C8Q,C67R,C84N; PDB code 1r28; Ahmad *et al.*, 2003). Cysteine S atoms are highlighted in magenta. A $2|F_{\rm o}| - |F_{\rm c}|$ electron-density map corresponding to the wild-type BCL6 POZ domain data, contoured to 1.5σ, is shown in blue.

one of the $\beta1$–$\beta5'$ β-sheets. The structure of the mutant BCL6 POZ domain in complex with either SMRT or BCoR revealed corepressor contacts involving both the main chain and side chain of the mutated residue 8 (Ahmad *et al.*, 2003; Ghetu *et al.*, 2008); the effect of Cys8 mutation on corepressor interactions remains to be determined.

Cys67 is located in the loop between $\alpha3$ and $\beta4$ at the top of the BCL6 POZ-domain dimer (Figs. 1 and 2). This region is highly flexible and the corresponding loop of the Miz-1 POZ domain undergoes significant rearrangement when Miz-1 POZ dimers associate into tetramers (Stead *et al.*, 2007). Tetramerization of the Miz-1 POZ domain is mediated *via* the interaction of dimers at the exposed $\beta3$–$\beta2$–$\beta4$ sheets located at the top of each subunit; this interaction results in the displacement of an outer $\beta4$ strand from one subunit of each constituent dimer, with the $\alpha3$–$\beta4$ loop being repositioned to reside adjacent to the β-sheet tetramerization interface. Although it is not currently known whether the BCL6 POZ-domain dimer uses a similar interface for higher order homo- or hetero-oligomerization, it will now be relevant to evaluate the effect of the C67R mutation on POZ-domain interactions involving this region.

The crystal structure of the wild-type BCL6 POZ domain confirms previously reported structures of a mutant protein and shows that the C8Q, C67R and C84N mutations have no effect on the overall backbone conformation. It will now be pertinent to study the interaction of the wild-type POZ domain both with transcriptional co-regulators and with other POZ partners. Knowledge of the structure of the wild-type BCL6 POZ domain will have direct relevance for the design of therapeutics that target its interactions in B-cell lymphoma.

This work was funded by Yorkshire Cancer Research. We thank staff at the Diamond Synchrotron Light Source (Didcot, UK) and Dr Arwen Pearson (University of Leeds) for assistance during X-ray data collection.

References

Ahmad, K. F., Engel, C. K. & Privé, G. G. (1998). *Proc. Natl Acad. Sci. USA*, **95**, 12123–12128.

Ahmad, K. F., Melnick, A., Lax, S., Bouchard, D., Liu, J., Kiang, C. L., Mayer, S., Takahashi, S., Licht, J. D. & Privé, G. G. (2003). *Mol. Cell*, **12**, 1551–1564.

Baron, B. W., Desai, M., Baber, L. J., Paras, L., Zhang, Q., Sadhu, A., Duguay, S., Nucifora, G., McKeithan, T. W. & Zeleznik-Le, N. (1997). *Genes Chromosomes Cancer*, **19**, 14–21.

Baron, B. W., Nucifora, G., McCabe, N., Espinosa, R. III, Le Beau, M. M. & McKeithan, T. W. (1993). *Proc. Natl Acad. Sci. USA*, **90**, 5262–5266.

Britton, D. (1972). *Acta Cryst.* A**28**, 296–297.

Cattoretti, G., Chang, C. C., Cechova, K., Zhang, J., Ye, B. H., Falini, B., Louie, D. C., Offit, K., Chaganti, R. S. & Dalla-Favera, R. (1995). *Blood*, **86**, 45–53.

Chang, C. C., Ye, B. H., Chaganti, R. S. & Dalla-Favera, R. (1996). *Proc. Natl Acad. Sci. USA*, **93**, 6947–6952.

Chattopadhyay, A., Tate, S. A., Beswick, R. W., Wagner, S. D. & Ko Ferrigno, P. (2006). *Oncogene*, **25**, 2223–2233.

Chen, S. J., Zelent, A., Tong, J. H., Yu, H. Q., Wang, Z. Y., Derre, J., Berger, R., Waxman, S. & Chen, Z. (1993). *J. Clin. Invest.* **91**, 2260–2267.

Collaborative Computational Project, Number 4 (1994). *Acta Cryst.* D**50**, 760–763.

Davis, I. W., Leaver-Fay, A., Chen, V. B., Block, J. N., Kapral, G. J., Wang, X., Murray, L. W., Arendall, W. B. III, Snoeyink, J., Richardson, J. S. & Richardson, D. C. (2007). *Nucleic Acids Res.* **35**, W375–W383.

DeLano, W. L. (2002). *The PyMOL Molecular Graphics System.* http://www.pymol.org.

Emsley, P. & Cowtan, K. (2004). *Acta Cryst.* D**60**, 2126–2132.

French, S. & Wilson, K. (1978). *Acta Cryst.* A**34**, 517–525.

Ghetu, A. F., Corcoran, C. M., Cerchietti, L., Bardwell, V. J., Melnick, A. & Privé, G. G. (2008). *Mol. Cell*, **29**, 384–391.

Huynh, K. D. & Bardwell, V. J. (1998). *Oncogene*, **17**, 2473–2484.

Kantardjieff, K. A. & Rupp, B. (2003). *Protein Sci.* **12**, 1865–1871.

Kelly, K. F. & Daniel, J. M. (2006). *Trends Cell Biol.* **16**, 578–587.

Kerckaert, J. P., Deweindt, C., Tilly, H., Quief, S., Lecocq, G. & Bastard, C. (1993). *Nature Genet.* **5**, 66–70.

Laskowski, R. A., MacArthur, M. W., Moss, D. S. & Thornton, J. M. (1993). *J. Appl. Cryst.* **26**, 283–291.

Leslie, A. G. W. (1992). *Jnt CCP4/ESF–EACBM Newsl. Protein Crystallogr.* **26**.

Li, X., Peng, H., Schultz, D. C., Lopez-Guisa, J. M., Rauscher, F. J. III & Marmorstein, R. (1999). *Cancer Res.* **59**, 5275–5282.

Maeda, T., Hobbs, R. M. & Pandolfi, P. P. (2005). *Cancer Res.* **65**, 8575–8578.

Maiti, R., Van Domselaar, G. H., Zhang, H. & Wishart, D. S. (2004). *Nucleic Acids Res.* **32**, W590–W594.

Murshudov, G. N., Vagin, A. A. & Dodson, E. J. (1997). *Acta Cryst.* D**53**, 240–255.

Navaza, J. (2001). *Acta Cryst.* D**57**, 1367–1372.

Parekh, S., Polo, J. M., Shaknovich, R., Juszczynski, P., Lev, P., Ranuncolo, S. M., Yin, Y., Klein, U., Cattoretti, G., Dalla Favera, R., Shipp, M. A. & Melnick, A. (2007). *Blood*, **110**, 2067–2074.

Parekh, S., Privé, G. & Melnick, A. (2008). *Leuk. Lymphoma*, **49**, 874–882.

Phan, R. T. & Dalla-Favera, R. (2004). *Nature (London)*, **432**, 635–639.

Phan, R. T., Saito, M., Basso, K., Niu, H. & Dalla-Favera, R. (2005). *Nature Immunol.* **6**, 1054–1060.

Polo, J. M., Dell'Oso, T., Ranuncolo, S. M., Cerchietti, L., Beck, D., Da Silva, G. F., Privé, G. G., Licht, J. D. & Melnick, A. (2004). *Nature Med.* **10**, 1329–1335.

Ranuncolo, S. M., Polo, J. M., Dierov, J., Singer, M., Kuo, T., Greally, J., Green, R., Carroll, M. & Melnick, A. (2007). *Nature Immunol.* **8**, 705–714.

Rees, D. C. (1980). *Acta Cryst.* A**36**, 578–581.

Schubot, F. D., Tropea, J. E. & Waugh, D. S. (2006). *Biochem. Biophys. Res. Commun.* **351**, 1–6.

Stead, M. A., Trinh, C. H., Garnett, J. A., Carr, S. B., Baron, A. J., Edwards, T. A. & Wright, S. C. (2007). *J. Mol. Biol.* **373**, 820–826.

Steczko, J., Donoho, G. A., Dixon, J. E., Sugimoto, T. & Axelrod, B. (1991). *Protein Expr. Purif.* **2**, 221–227.

Stogios, P. J., Chen, L. & Privé, G. G. (2007). *Protein Sci.* **16**, 336–342.

Stogios, P. J., Downs, G. S., Jauhal, J. J., Nandra, S. K. & Privé, G. G. (2005). *Genome Biol.* **6**, R82.

Ye, B. H., Chaganti, S., Chang, C. C., Niu, H., Corradini, P., Chaganti, R. S. & Dalla-Favera, R. (1995). *EMBO J.* **14**, 6209–6217.

Ye, B. H., Lista, F., Lo Coco, F., Knowles, D. M., Offit, K., Chaganti, R. S. & Dalla-Favera, R. (1993). *Science*, **262**, 747–750.